

## **Section 9**

Development of and studies with coupled and Earth system models and data assimilation systems.



# Indian rainfall and Eurasian snow climatology in CMIP5 historical simulations

Amita Prabhu<sup>1,\*</sup> and Sujata K. Mandke<sup>1</sup>

<sup>1</sup>Indian Institute of Tropical Meteorology, Dr. Homi Bhabha Road, Pashan, Pune-411008, INDIA  
\*[amitaprabhu@tropmet.res.in](mailto:amitaprabhu@tropmet.res.in), [amin@tropmet.res.in](mailto:amin@tropmet.res.in)

## 1. Introduction

The interannual variations (IAV) of the Indian summer monsoon rainfall (ISMR) have a very large impact on the agriculture and economy of the country. The understanding and prediction of ISMR is thus extremely important and have been a subject of considerable urgency. The IAV of ISMR are significantly correlated with the tropical sea surface temperature and snow cover anomalies. An inverse relation between Eurasian/Himalayan snow extent/depth in the preceding season and ISMR has been extensively documented (Hahn and Shukla, 1976; Kripalani and Kulkarni, 1999 and many others). As the continental snow cover is one of the few potential sources of seasonal persistence in the Asian region, the snow-monsoon connection is especially compelling. Of late, many international climate research groups made an extensive set of climate runs as a part of Coupled Model Intercomparison Project phase 5 (CMIP5) explorations (Taylor et al., 2012). CMIP5 provides a promising opportunity to examine snow-monsoon links simulated by several state-of-the-art global atmosphere-ocean coupled models. The simulation of better rainfall climatology has proven to be a test of model's ability to simulate IAV (Sperber and Palmer, 1996). Therefore, as an initial step towards the goal of studying snow-monsoon relation, we assess fidelity of five CMIP5 models to simulate climatology of precipitation averaged over Indian land (INDP) and snow averaged over Eurasian (EURS) region (20-140°E, 50-70°N) in historical runs of five CMIP5 models (Table 1).

**Table 1:** CMIP5 models used in the present study (horizontal resolution (in ° E X ° N))

No.	Model name	Atmospheric horizontal resolution
1.	CCSM4	1.2x0.9
2.	CNRM-CM5	1.4x1.4
3.	GFDL-ESM2G	2.5x2.0
4.	MIROC4h	T213L56
5.	NorESM1-M	2.5x1.9

## 2. Data

The model data from CMIP5 historical simulations (<http://pcmdi3.llnl.gov/esgcat/home.htm>) is used. The information on individual models is available (<http://cmip-pcmdi.llnl.gov/cmip5/>). The model simulations are validated using the corresponding observations - (i) High resolution (0.25° x 0.25°) spatially gridded rainfall data developed by India Meteorological Department (Pai et al., 2014) (ii) Snow water equivalent (SWE) data obtained from the Nimbus-7 Scanning Multi-Channel Microwave Radiometer and Defense Meteorological Satellite Program's Special Sensor Microwave Imager and archived at the National Snow and Ice Data Center (<ftp.sidacs.colorado.edu>). SWE is hereinafter referred to simply as snow in this study. Model and observed climatologies are based on the period 1979-2006, which is a consistent available data record across all data sets used.

## 3. Results

The annual cycles of INDP (Figure 1a) and EURS (Figure 1b) for five selected CMIP5 models along with the corresponding observations are depicted. There is a general consensus among model simulations and observations in regard to representing annual cycle of INDP except MIROC4h model that overestimates precipitation and also exhibits much earlier monsoon onset as compared to the observed data. All models simulate excessive (deficient) EURS during January-March (September-October) (Figure 1b). Next, summer averaged INDP and winter averaged EURS climatologies of five CMIP5 models are compared with observations (Figure 2). The summer season is considered from June to September and the winter season is from December of the previous year to January- March of the next year. All five models underestimate winter EURS climatology. Further, the summer INDP climatology simulated by three models exceeds observations, being less than observations for CNRM-CM5 model and in good agreement with observations for GFDL-ESM2G model.

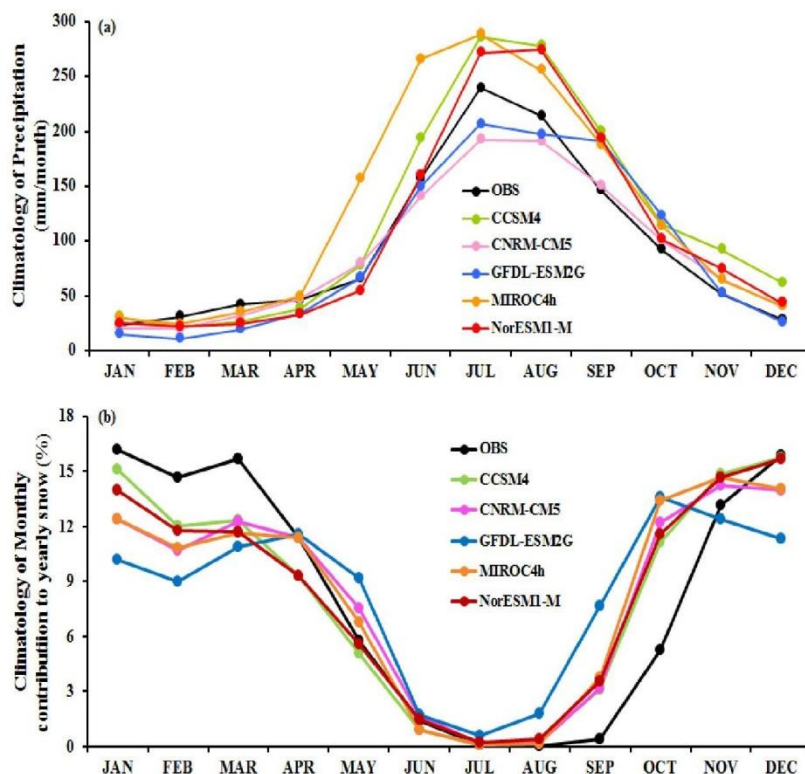


**Figure 1: (a) Monthly mean precipitation climatology averaged over Indian land; (b) Monthly mean snow climatology averaged over Eurasia**

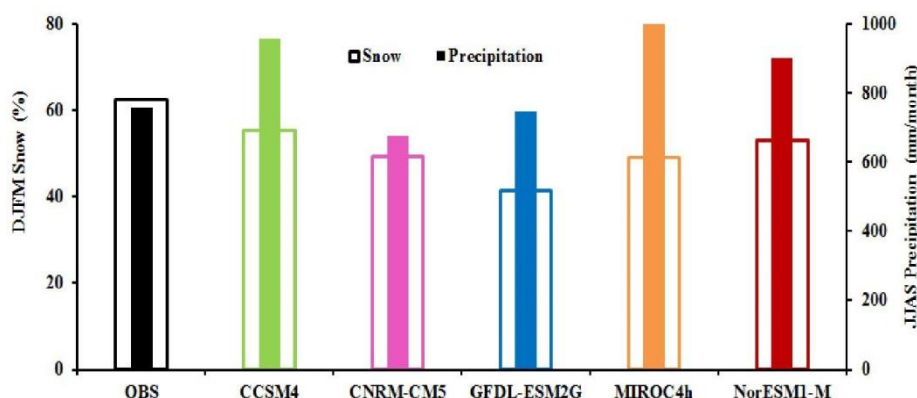


**Figure 2: Summer mean precipitation climatology averaged over Indian land and winter mean snow climatology averaged over Eurasia**

## References

- Hahn D.J., Shukla J. (1976) An apparent relation between Eurasian snow cover and Indian monsoon rainfall. *J. Atmos Sci*, 33:2461–2462
- Kripalani R.H., Kulkarni A. (1999) Climatology and variability of historical Soviet snow depth data: some new perspectives in snow-Indian monsoon teleconnections. *Clim Dyn*, 15:475–489
- Pai D.S., Sridhar L., Rajeevan M., Sreejith O.P., Satbhai N.S., Mukhopadhyay B. (2014) Development of a new high spatial resolution (0.25 × 0.25 degree) long period (1901–2010) daily gridded rainfall data set over India and its comparison with existing data sets over the region. *Mausam*, 65(1):1–18
- Sperber K.R., Palmer T.N. (1996) Interannual tropical rainfall variability in general circulation model simulations associated with the AMIP. *J Clim*, 9 (11) : 2727–2750
- Taylor, K.E., Stouffer, R.J. and Meehl, G.A. (2012) An overview of CMIP5 and the experiment design, *Bull. Amer. Meteorol. Soc*, 90,4 85–498.

# Preliminary numerical experiments on the prediction of Typhoon Lionrock (2016) using the global atmosphere-ocean coupled model

Akiyoshi Wada\*, Hiromasa Yoshimura and Masayuki Nakagawa  
 Meteorological Research Institute, Tsukuba, Ibaraki, 305-0052, JAPAN  
 \*awada@mri-jma.go.jp

## 1. Introduction

Previous studies have reported that typhoons tended to be overdeveloped compared with the best-track analysis when the intensity was predicted using the 7-km mesh nonhydrostatic global spectral atmospheric Double Fourier Series Model (DFSM) (Nakano et al., 2017). In addition, the typhoon intensity predicted by DFSM was sensitive to surface boundary (Wada et al., 2018a) and cloud-physics scheme (Wada et al., 2018b) incorporated into the DFSM. Aside from this fact, it is known that sea surface cooling caused by typhoons helps suppress the overdevelopment of typhoons. However, it is necessary to use a global atmosphere-ocean coupled model to introduce the negative-feedback effect. In this report, preliminary numerical simulations were performed on Typhoon Lionrock (2016) by using the DFSM-based 7-km mesh global atmosphere model coupled with the MRI Community Ocean Model Version 4.4 (MRI.COM). The MRI.COM has been developed for contributing the projects of the Coupled Model Intercomparison Project (CMIP) phases (<https://cera-www.dkrz.de/WDCC/ui/cersearch/cmip6?input=CMIP6>. CMIP.MRI.MRI-ESM2-0). The purpose of this study is to understand the impact of cloud physics and cumulus parameterization on the typhoon simulations in a coupled atmosphere and ocean framework.

## 2. Experimental design

The initial time of the prediction of Lionrock is set to 0000 UTC 23 August 2016. The prediction period is from this initial time to 0000 UTC 31 August 2016. The integration time is 8 days. Table 1 shows a list of sensitivity numerical experiments for the prediction of Lionrock. The DFSM-based 7-km mesh global atmosphere model is almost the same as that used in Wada et al (2018a). The MRI.COM is a free-surface, depth-coordinate ocean-ice model that solves primitive equations using Boussinesq and hydrostatic approximation in a tripolar grid system. The horizontal grid arrangement is primarily 0.5-degree latitude/1-degree longitude with meridional refinement down to 0.3 degree within 10 degrees north and south of the equator. The number of the vertical level is 61 with a top grid cell of 0-2 m. The Japan Meteorological Agency 6-hourly global objective analysis data are used for each experiment to derive atmospheric initial conditions (Nakano et al., 2017). In addition, the global ocean reanalysis data are used for each experiment to derive oceanic initial conditions (Toyoda, private communication).

Table 1 List of sensitivity numerical experiments for the prediction of Lionrock

Experiment name	Cloud physics	Cumulus parameterization
NSMITH	Smith (1990)	×
NTDK	Tiedtke(1993)	×
ASSMITH	Smith (1990)	Randall and Pan (1993)

## 3. Results

### 3.1 Track and SST simulations

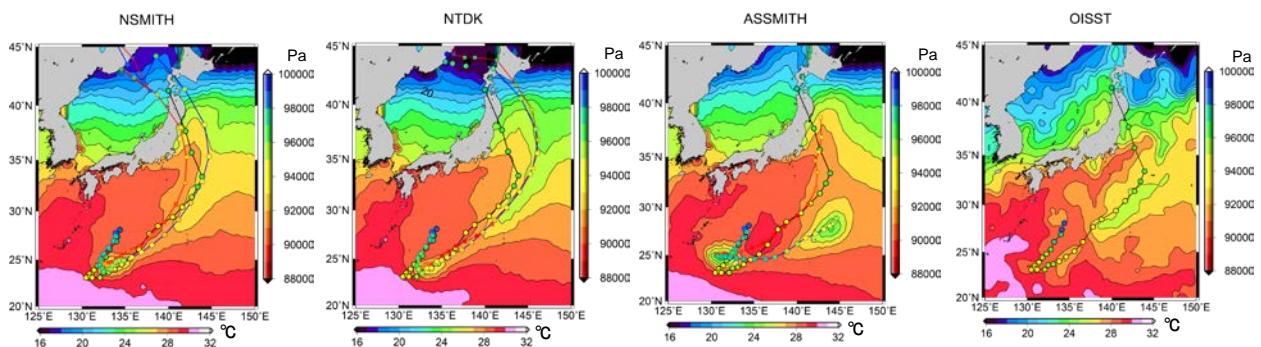


Figure 1 Horizontal distributions of simulated sea surface temperature in (a) NSMITH, (b) NTDK and (c) ASSMITH experiments and (d) analyzed sea surface temperature (colors with the contours (1 °C) on 0000 UTC 31 August with the best track (the color within a circle indicates central pressures) and simulated tracks (red: results by DFSM alone, blue: results by the coupled model) in (a) NSMITH, (b) NTDK and (c) ASSMITH experiments.

Figures 1a-c show the horizontal distributions of simulated sea surface temperature in (a) NSMITH, (b) NTDK and (c) ASSMITH experiments together with the simulated tracks and the analyzed best track. The Regional Specialized Meteorological Center Tokyo best-track analysis is used as the analyzed best track in this study. Sea surface cooling areas induced by simulated Lionrock are found just after the recurvature and along the right side of the track afterward in the NSMITH and NTDK experiments, while the areas are clear before the recurvature and around 27.5°N, 145°E in the ASSMITH experiment. The locations of the simulated sea surface cooling areas are consistent with the analyzed sea surface temperature field (Fig. 1d). It is interesting to note that ASSMITH experiments alone have large differences in simulated tracks between the atmosphere-ocean coupled model experiment and the DFSM-alone experiment. It is suggested that the typhoon tracks simulated with the cumulus parameterization are highly influenced by ocean coupling.

### 3.2 Intensity simulations

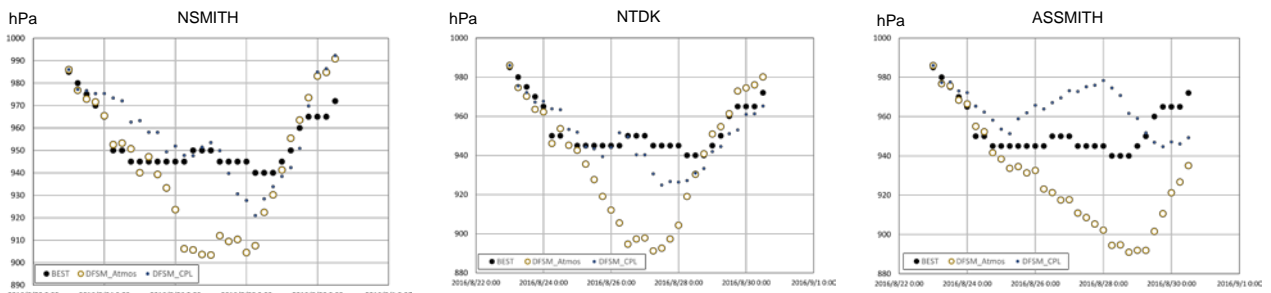


Figure 2 Time series of best-track (BEST) and simulated central pressures in (a) NSMITH, (b) NTDK and (c) ASSMITH experiments. 'DFSM\_Atmos' indicates the central pressures simulated by the DFSM-alone model, while 'DFSM\_CPL' indicates the central pressures simulated by the atmosphere-ocean coupled model.

Figure 2 shows the time series of best-track and simulated central pressures in (a) NSMITH, (b) NTDK and (c) ASSMITH experiments. During the early intensification phase, the Smith cloud physics scheme is highly sensitive of simulated central pressure to ocean coupling. The simulated typhoon in the NSMITH and NTDK experiments continued to intensify even around 0000 UTC on 28 August, while the simulated typhoon became weakened after 0000 TUTC on 25 August to 0000 UTC on 28 August and then intensified again in the ASSMITH experiment. It should be noted that the tracks quite differ between the atmosphere-ocean coupled model experiment and the DFSM-alone experiment. However, the effect of ocean coupling on simulated central pressures becomes much clearer during the late intensification and mature phases, which is different from the effect reported in the previous studies (e.g., Wada et al., 2018c).

### 4. Future subject

The cumulus parameterization used in the Meteorological Research Institute Earth System Model version 2.0 (MRI-ESM2.0) is not based on the Arakawa-Schubert cumulus parameterization (Randall and Pan, 1993) but based on Yoshimura et al. (2015). However, the 7-km mesh DFSM with the cumulus parameterization of Yoshimura et al. (2015) also tends to overdevelop the intensity of typhoons (not shown). It is a future subject to clarify whether the influence of sea surface cooling simulated by the atmosphere-ocean coupled model on typhoon prediction depends on the formulation in each scheme or the concept of cumulus parameterization itself.

### References

- Nakano, M., Wada, A., Sawada, M., Yoshimura, H., Onishi, R., Kawahara, S., Sasaki, W., Nasuno, T., Yamaguchi, M., Iriguchi, T., Sugi, M., and Takeuchi, Y. (2017). Global 7 km mesh nonhydrostatic Model Intercomparison Project for improving TYphoon forecast (TYMIP-G7): experimental design and preliminary results. *Geosci. Model Dev.*, 10, 1363-1381, <https://doi.org/10.5194/gmd-10-1363-2017>
- Randall, D. and Pan D.-M. (1993). Implementation of the Arakawa-Schubert cumulus parameterization with a prognostic closure: The representation of cumulus convection in numerical models, *AMS Meteor. Monogr. Series*, 46, 137-144.
- Smith, R. N. B. (1990). A scheme for predicting layer clouds and their water content in a general circulation model, *Q. J. Roy. Meteor. Soc.*, 116, 435-460.
- Tiedtke, M., (1993). Representation of clouds in large scale models. *Mon. Wea. Rev.*, 121, 3040-3061.
- Wada, A., H. Yoshimura, and M. Nakagawa (2018a). Sensitivity of the prediction of Typhoon Lionrock (2016) to the surface boundary scheme using the 7-km mesh nonhydrostatic global spectral atmospheric Double Fourier Series Model (DFSM). *CAS/JSC WGNE Res. Activities in Atm. And. Oceanic Modelling. Rep.* 48, 4-13.
- Wada, A., H. Yoshimura, and M. Nakagawa (2018b). Sensitivity of the prediction of Typhoon Lionrock (2016) to the parameter in the cloud scheme using the 7-km mesh nonhydrostatic global spectral atmospheric Double Fourier Series Model (DFSM). *CAS/JSC WGNE Res. Activities in Atm. And. Oceanic Modelling. Rep.* 48, 4-11.
- Wada, A., S. Kanada, and H. Yamada (2018c). Effect of air-sea environmental conditions and interfacial processes on extremely intense typhoon Haiyan (2013). *J. Geophys. Res.*, 123, 10379-10405. <https://doi.org/10.1029/2017JD028139>.
- Yoshimura, H., R. Mizuta, and H. Murakami (2015). A spectral cumulus parameterization scheme interpolating between two convective updrafts with semi-Lagrangian calculation of transport by compensatory subsidence. *Mon. Wea. Rev.*, 143, 597-621, doi:10.1175/MWR-D-14-00068.1.

### Acknowledgements

This work was supported by JSPS KAKENHI Grant Number JP15K05292.

# The impacts of a cold eddy induced by Typhoon Trami (2018) on the intensity forecast of Typhoon Kong-Rey (2018)

Akiyoshi Wada

Meteorological Research Institute, Tsukuba, Ibaraki, 305-0052, JAPAN

\*awada@mri-jma.go.jp

## 1. Introduction

A tropical depression was upgraded to a tropical cyclone around 12.6°N, 142.6°E at 06 UTC on 29 September in 2018 and was named Kong-Rey (2018). According to the Regional Specialized Meteorological Center (RSMC) Tokyo best track analysis, the central pressure reached 900 hPa at 12 UTC on 1 October around 16.8°N, 134.4°E. Kong-Rey had kept the intensity for 18 hours and then its central pressure rapidly increased by 940 hPa for the subsequent 12 hours, like Typhoon Trami (2018) (Wada, 2019). Kong-Rey moved to follow Trami after a week, but no redevelopment like Trami was analyzed in the RSMC best track data. In fact, unlike Trami, Kong-Rey passed over an oceanic cold eddy induced by the passage of Trami. Figure 1 shows the horizontal distributions of sea surface temperature (SST) at 12 UTC on 29 September in 2018. One is obtained from the Merged Satellite and In-situ Data Global Daily Sea Surface Temperatures (MGDSST) data set with the horizontal resolution of 0.25° (Kurihara et al., 2006) (Fig. 1a) and the other is obtained from Microwave Optimally Interpolated Sea Surface Temperatures (OISST) data set with the horizontal resolution of 0.25° (<http://www.remss.com/measurements/sea-surface-temperature/oisst-description/>) (Fig. 1b). The representation of sea surface cooling (SSC) induced by Trami is much different between the two data sets.

The purpose of this study is to clarify the impacts of the cold eddy induced by Trami on the intensify forecast of Kong-Rey. Numerical simulations were performed with two different oceanic initial conditions obtained from MDGSST and OISST and a 2 km-mesh nonhydrostatic atmosphere model coupled with ocean surface wave and multilayer ocean models (Wada et al., 2010, 2018) with the Japan Meteorological Agency (JMA) global objective analysis with horizontal resolution of 20 km and the JMA North Pacific Ocean analysis with horizontal resolution of 0.5°. In addition, sensitivity numerical experiments were conducted with the oceanic initial condition at 12 UTC on 29 September merged with an artificial cold vortex centered at 21°N, 129°E, which is the same procedure as Wada (2019). The initial time, corresponding to the time of atmospheric initial condition, and integration period are 12 UTC on 29 September and 144 hours with the time interval of 3 seconds.

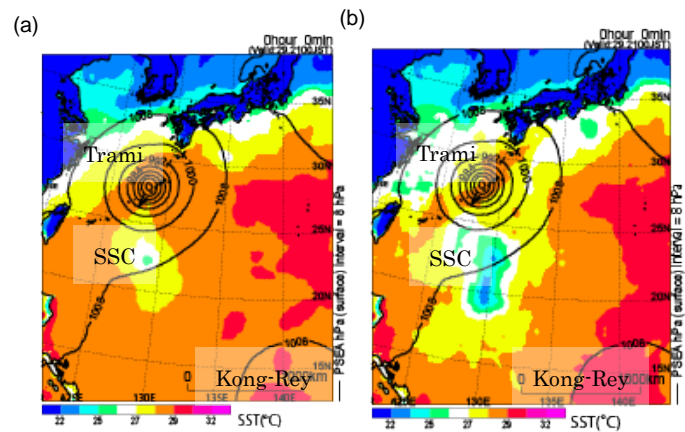


Figure 1. Horizontal distributions of sea-level pressures at the interval of 8 hPa and SST obtained from (a) MGDSSST and (b) OISST datasets at 12 UTC on 29 September in 2018.

## 2. Experimental design

The list of numerical simulations is shown in Table 1. Four numerical simulations were performed in this study. The model physics in the coupled model is the same as Wada (2019): That includes an explicit three-ice bulk microphysics scheme, turbulent closure model in the atmospheric boundary layer, a radiation scheme, roughness lengths based on the third-generation ocean surface wave model and a sea spray parameterization. These are the same as Wada et al. (2018). No cumulus parameterization was used in this study.

Table1 List of numerical simulations

Name	Model	Oceanic initial data	Additional information
MGDSST	Coupled NHM-wave-ocean	MGDSST+JMA analysis	
OISST	Coupled NHM-wave-ocean	OISST+JMA analysis	
MGDSST_COLD	Coupled NHM-wave-ocean	MGDSST+JMA analysis	+Artificial cold eddy
OISST_COLD	Coupled NHM-wave-ocean	OISST+JMA analysis	+Artificial cold eddy

## 3. Results

Figure 2 shows the results of track simulations and the RSMC best-track together with the horizontal distribution of SST obtained from OISST on 3 October in 2018. The model used in this study reasonably simulated the track of Kong-Rey although the track excessively moved westward north of 20°N. The effect of ocean coupling on the track simulation was negligibly small although SSC was clearly seen along the track. All the results regarding the track simulations are consistent with those in Wada (2019).

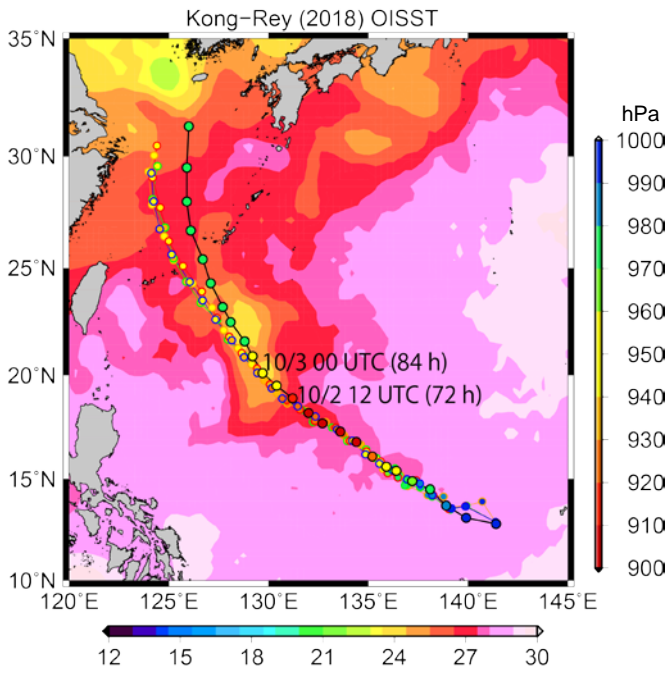


Figure 2. Results of track simulations together with the best-track analysis. Colors within the circles indicate the value of the central pressure. Color lines indicate the result of OISST (orange), MGDSST (green), OISST\_COLD (red) and MGDSST\_COLD (blue), respectively. Color shades indicate SST obtained from the OISST data set.

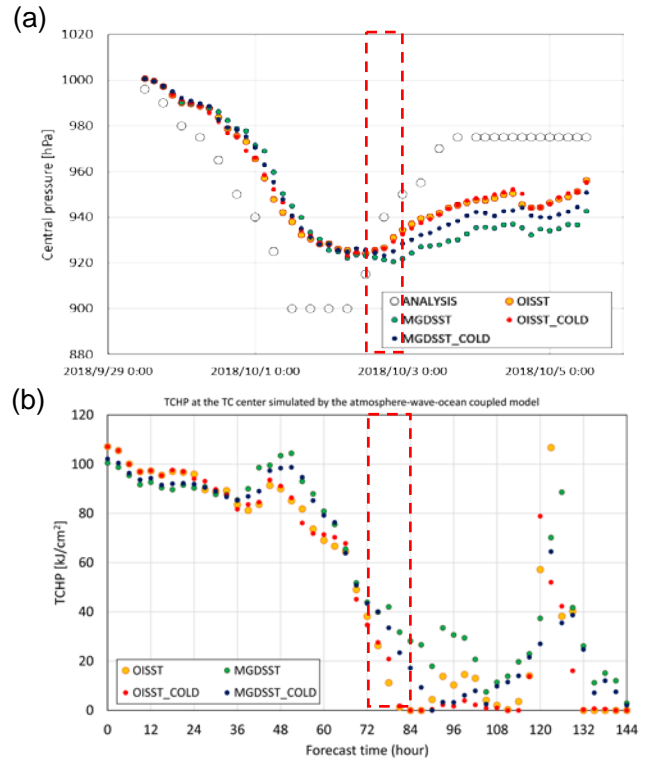


Figure 3. Time series of (a) the best-track analyzed central pressure and simulated central pressures and (b) tropical cyclone heat potential at the location of the simulated storm center. Dashed boxes indicate the period from 2 (72-hour integration time) to 3 (84-hour integration time) October.

Figure 3a shows the time series of simulated central pressures together with the best-track central pressure. The coupled model hardly simulated the minimum central pressure of Kong-Rey in all four simulation experiments. In addition, the coupled model hardly simulated rapid increase in the central pressure from 2 to 3 October. The effect of the artificial cold eddy on the central pressure simulation was significant when MGDSST was used, while that was not clear when OISST was used. This was because the SST at the initial time obtained from OISST data set was so low compared with the SST obtained from MGDSST that tropical cyclone heat potential (TCHP, Wada et al., 2018) at the center of the simulated storm rapidly decreased from 2 (72-hour integration time) to 3 (84-hour integration time) October (Fig. 3b). The difference of TCHPs between MGDSST and MGDSST\_COLD experiments was much larger than that between OISST and OISST\_COLD experiments, which is consistent with the result of central pressure simulations (Fig. 3a). The differences also affected the net heat flux (summation of solar radiation, long-wave radiation sensible heat and latent heat flux) transported from the ocean to the atmosphere within a radius of 50 km from the storm center (not shown). In fact, the value of TCHP in the OISST\_COLD experiment was almost the same as that in the OISST experiment. The artificial cold eddy could not contribute to further increasing the simulated central pressures and improve the intensity prediction of Kong-Rey, which is different from Trami (Wada, 2019).

#### 4. Concluding remarks

Unlike the concluding remarks in Wada (2019), this study has shown that there is a limit to the improvement of typhoon prediction by improving the ocean initial condition. It is necessary to improve not only ocean coupling prediction system but also the atmospheric initial conditions and the physical processes in the atmosphere model to improve the prediction of rapid decaying of typhoons.

#### References

- Kurihara, Y., T. Sakurai, and T. Kuragano (2006). Global daily sea surface temperature analysis using data from satellite microwave radiometer, satellite infrared radiometer and in-situ observations (in Japanese). *Wea. Service Bull.*, 73, 1–18.
- Wada, A (2019). The impacts of preexisting oceanic cold eddies on the intensity forecast of Typhoon Trami (2018) during the mature phase. *Research Activities in Atmospheric and Oceanic Modelling*, 49, in print.
- Wada, A., N. Kohno and Y. Kawai (2010). Impact of wave-ocean interaction on Typhoon Hai-Tang in 2005. *SOLA*, 6A, 13-16.
- Wada, A., S. Kanada, and H. Yamada (2018). Effect of air-sea environmental conditions and interfacial processes on extremely intense typhoon Haiyan (2013). *Journal of Geophysical Research: Atmospheres*, 123, 10379-10405.

#### Acknowledgements

This work was supported by JSPS KAKENHI Grant Number JP15K05292 and JP17H02964.

# Roles of ocean coupling and cumulus parameterization in predicting rainfall amounts caused by landfalling typhoons in the Philippines

Akiyoshi Wada<sup>1</sup>, Robb P. Gile<sup>2</sup>

<sup>1</sup>Meteorological Research Institute, Tsukuba, Ibaraki, 305-0052, JAPAN

<sup>2</sup>Philippine Atmospheric, Geophysical and Astronomical Services Administration,  
Diliman, Quezon City 1100, PHILIPPINES

<sup>1</sup>awada@mri-jma.go.jp

## 1. Introduction

In the Philippines, 4-5 typhoons make landfall in a year on average. Climatologically, typhoons tend to pass through the central and southern parts of the Philippines in December. Since the heavy rainfall associated with the typhoons sometimes cause floods and thereby natural disasters in these areas, it is urgent to establish numerical forecasting particularly for heavy rainfall associated with the typhoons and to improve the accuracy of the rainfall forecast.

The purpose of this study is to evaluate the applicability of a nonhydrostatic atmosphere model (NHM) for rainfall forecasts associated with landfalling typhoons in the Philippines. This study addressed typhoons Kai-Tak, Tembin in 2017 and Sanba in 2018. Numerical simulations on these typhoons were performed by NHM and the atmosphere- wave-ocean coupled model (Wada et al., 2010, 2018) with a horizontal resolution of 3 km. We compared rainfall simulations by the model without any cumulus parameterizations with those with the Kain-Fritsch cumulus parameterization (KF) (Kain and Fritsch, 1990).

## 2. Experimental design

The list of numerical simulations is shown in Table 1. The initial time was 0000 UTC on 14 December in 2017 for Kai-Tak, 0000 UTC on 21 December in 2017 for Tembin, and 0000 UTC on 11 February in 2018 for Sanba. The computational domain was the same for three typhoon cases (Figure 1): The domain was 2520 x 2520 km. The number of vertical layers was 55. The top height was approximately 27 km.

The integration time was 72 hours. The time step was 6 seconds for NHM, 36 seconds for the ocean model, and 6 minutes for the ocean surface wave model. The physical components were exchanged between NHM, the ocean model, and the ocean surface wave model every time step of the model with a longer time step. The Japan Meteorological Agency (JMA) global objective analysis with horizontal resolution of 20 km and the JMA North Pacific Ocean analysis with horizontal resolution of 0.5° were used for creating atmospheric and oceanic initial conditions and atmospheric lateral boundary conditions.

The daily accumulated rainfall amount obtained by numerical simulations was verified against in-situ (raingauge) observations. Standard deviation, simulation bias to observation, correlation coefficient, bias score and equitable threat score were calculated. Climatological relative frequency was calculated based on all in-situ raingauge observations of three typhoon cases used in this study.

## 3. Results

Figure 2 shows the standard deviation, simulation bias to observation, and correlation coefficient of daily accumulated rainfall for 24 h, 48 h, and 72 h forecasts. Simulated daily accumulated rainfall was calculated as a difference between the precipitation accumulated by the moment in view and 24 hours before. The simulation bias to observation is equal to the slope of the linear regression. In conducting statistical analysis, daily accumulated precipitation data for the three typhoon cases are combined into one sample. Without the KF cumulus parameterization in the daily accumulated rainfall simulation, both the simulation bias and the correlation coefficient clearly decreased for 72 h forecasts in the A and AWO experiments although some improvement was found in the daily accumulated rainfall simulation connected with reducing the standard deviation. With the KF cumulus parameterization, the accuracy of the daily accumulated rainfall simulation was

Table 1 List of numerical simulations

Name	Model	Cumulus Parameterization	Typhoon cases
A	NHM	No	Kai-Tak
AWO	Coupled NHM-wave-ocean model	No	(2017/12/14/0000)
AKF	NHM	KF	Tembin
AWOKF	Coupled NHM-wave-ocean model	KF	(2017/12/21/0000)
			Sanba
			(2018/02/11/0000)

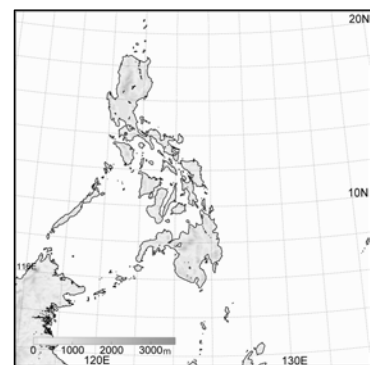


Figure 1. Computational domain.

sustained even for 72 h, while the accuracy for 24 h and 48 h forecasts was not better than that in the A and AWO experiments.

Figures 3 and 4 show the bias and equitable threat scores at 24 h, 48 h, and 72 h. The atmosphere-wave-ocean coupled model can contribute to improving the bias and equitable threat scores by quantitatively changing the simulated daily accumulated precipitation, particularly when the threshold of daily accumulated precipitation was small (Figure 4b). However, it is the cumulus convection parameterization that fundamentally changes the characteristics of the score.

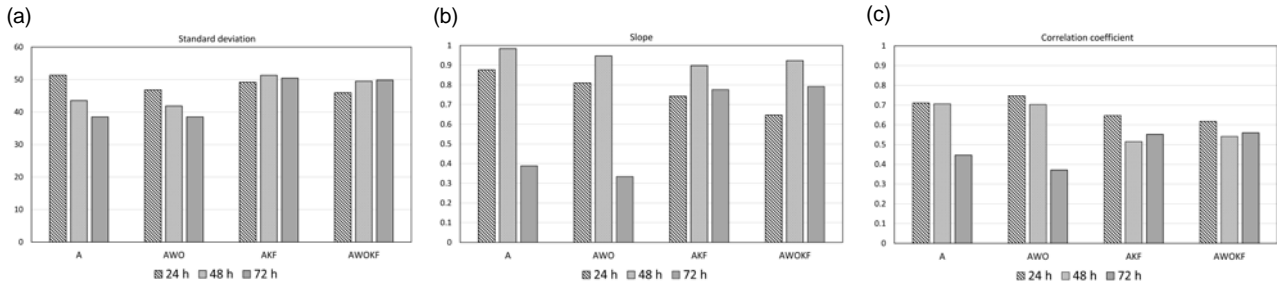


Figure 2 Standard deviation (a), simulation bias to observation (slope of the regression model) (b), and correlation coefficient (c) of daily accumulated rainfall at 24 h, 48 h, and 72 h.

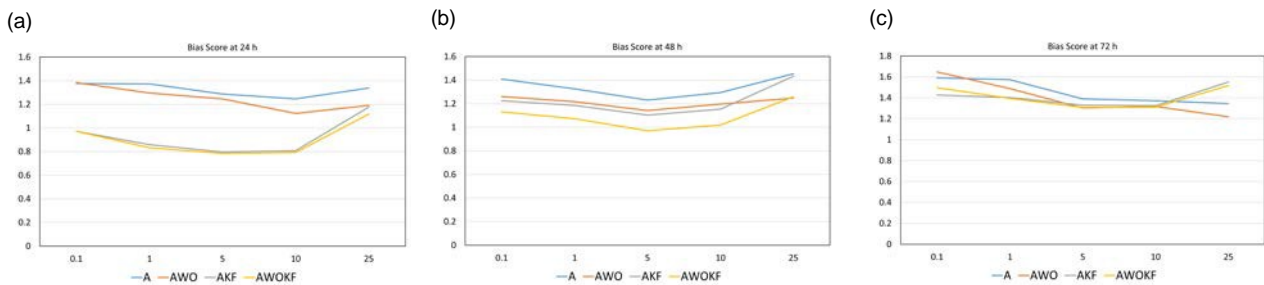


Figure 3 Bias score in each daily accumulated rainfall threshold of daily accumulated rainfall at 24 h (a), 48 h (b), and 72 h (c).

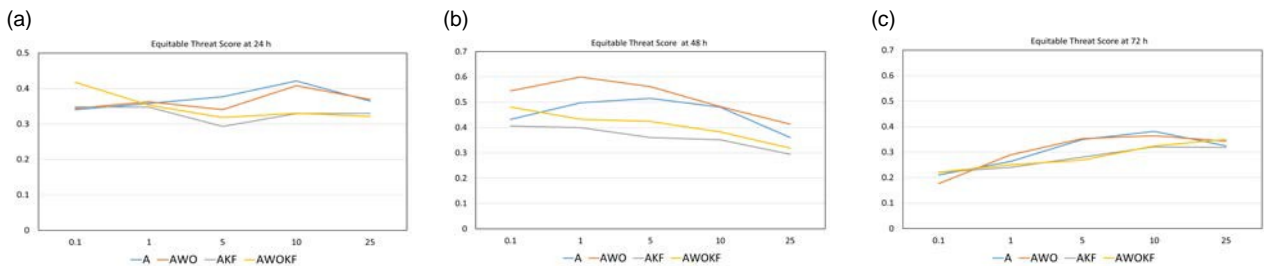


Figure 4 Equitable threat score in each daily accumulated rainfall threshold of daily accumulated rainfall at 24 h (a), 48 h (b), and 72 h (c).

#### 4. Concluding remarks

In numerical forecasting of heavy rains associated with typhoons making landfall in the Philippines, the forecast accuracy can be sustained at best only 48 hours when using the NHM without the KF cumulus parameterization. Even using the atmosphere-wave-ocean coupled model, the forecast accuracy cannot be fundamentally improved. As for the introduction of the KF cumulus parameterization in this study, it should be noted that it has been tuned to be optimized for heavy rainfalls around Japan. It is necessary to carry out suitable tuning for forecasting heavy rainfall associated with landfalling typhoons around the Philippines.

This verification result is only the result of numerical simulations with only one initial condition for each of three typhoon cases. From now on, it is necessary to increase the number of cases to verify. At that time, it may be sufficient to carry out numerical simulations with the NHM, not with the atmosphere-wave-ocean coupled model.

#### References

- Kain, J. S., and J. M. Fritsch (1990). A one-dimensional entraining/detraining plume model and its application in convective parameterization. *Journal of the Atmospheric Sciences*, 47, 2784-2802.
- Wada, A., N. Kohno and Y. Kawai (2010). Impact of wave-ocean interaction on Typhoon Hai-Tang in 2005. *SOLA*, 6A, 13-16.
- Wada, A., S. Kanada, and H. Yamada (2018). Effect of air-sea environmental conditions and interfacial processes on extremely intense typhoon Haiyan (2013). *Journal of Geophysical Research: Atmospheres*, 123, 10379-10405.

# The impacts of preexisting oceanic cold eddies on the intensity forecast of Typhoon Trami (2018) during the mature phase

Akiyoshi Wada

Meteorological Research Institute, Tsukuba, Ibaraki, 305-0052, JAPAN

\*awada@mri-jma.go.jp

## 1. Introduction

Typhoon Trami (2018) is one of the typhoons that made landfall in Japan. According to the Regional Specialized Meteorological Center (RSMC) Tokyo best track analysis, the central pressure reached 915 hPa at 18 UTC on 24 September around 20°N and then rapidly increased up to 950 hPa in 18 hours. After the rapid increases in the central pressure, intensity forecasts announced further intensification to 935 hPa, but the typhoon couldn't intensify again. In order to clarify the impact of the cold eddies over the ocean on this forecast error, we conducted numerical simulations with different oceanic initial conditions (daily oceanic analysis data from 19 to 25 September were used and the number of ensemble members is seven) using a 2 km-mesh nonhydrostatic atmosphere model coupled with ocean surface wave and multilayer ocean models (Wada et al., 2010, 2018) with the Japan Meteorological Agency (JMA) global objective analysis with horizontal resolution of 20 km and the JMA North Pacific Ocean analysis with horizontal resolution of 0.5°. In addition, a sensitivity numerical experiment was conducted with the oceanic initial condition on 23 September merged with an artificial cold vortex centered at 21°N, 129°E where both a mixed layer and thermocline were 50 m shallower than the initial field on 23 September used the control experiment. Moreover, ensemble simulations with a 2 km-mesh nonhydrostatic atmosphere model and seven different oceanic initial conditions were performed to compare the results with the ensemble simulations by the coupled model. The initial time, corresponding to the time of atmospheric initial condition, and the integration period are 00 UTC on 23 September and 180 hours with the time interval of 3 seconds.

## 2. Experimental design

The list of numerical simulations is shown in Table 1. Fifteen numerical simulations were performed in this study. The model physics in the coupled model includes an explicit three-ice bulk microphysics scheme, turbulent closure model in the atmospheric boundary layer, a radiation scheme, roughness lengths based on the third-generation ocean surface wave model and a sea spray parameterization. These are the same as in Wada et al. (2018). No cumulus parameterization was used in this study.

Figure 1 shows the computational domain and Figure 2 shows the horizontal distribution of tropical cyclone heat potential (Wada et al., 2012) in the AWO\_0923 (Fig. 2a) and AWO\_cold (Fig. 2b) experiments. A cold-eddy region in the AWO\_cold experiment was better reproduced than the region in the AWO\_0923 experiment around 21°N, 129°E.

Table 1 List of numerical simulations

Name	Model	Oceanic initial data	Additional information
[A/AWO]_0919	NHM/Coupled NHM-wave-ocean	19 September	[Noncouple/Couple]
[A/AWO]_0920	NHM/Coupled NHM-wave-ocean	20 September	Ensemble experiments
[A/AWO]_0921	NHM/Coupled NHM-wave-ocean	21 September	
[A/AWO]_0922	NHM/Coupled NHM-wave-ocean	22 September	
[A/AWO]_0923	NHM/Coupled NHM-wave-ocean	23 September	
[A/AWO]_0924	NHM/Coupled NHM-wave-ocean	24 September	
[A/AWO]_0925	NHM/Coupled NHM-wave-ocean	25 September	
AWO_cold	Coupled NHM-wave-ocean	23 September	+Artificial cold eddy

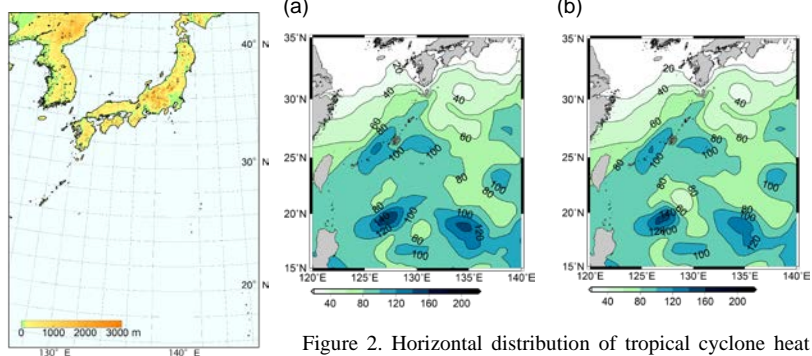


Figure 1. Computational domain.

Figure 2. Horizontal distribution of tropical cyclone heat potential (a) in the AWO\_0923 experiment and (b) in the AWO\_cold experiment.

## 3. Results

Figure 3 shows the results of track simulations in the A\_0923, AWO\_0923 and AWO\_cold experiments together with the best-track analysis. The model used in this study reasonably simulated the track of Trami although the track excessively moved westward around 20°N, 130°E. The effect of ocean coupling on the track simulation was negligibly small. In addition, the effect of oceanic cold eddy on the track simulation was also small. Compared with the operational forecast based on the results of the numerical prediction by the global atmospheric spectral model in the Japan Meteorological Agency, the track simulation was much improved due to the improvement of the

objective analysis with in situ observations by GPS dropsondes during the aircraft missions of the Tropical Cyclones-Pacific Asian Research Campaign for the Improvement of Intensity Estimations/Forecasts (T-PARCII, Ito et al., 2018).

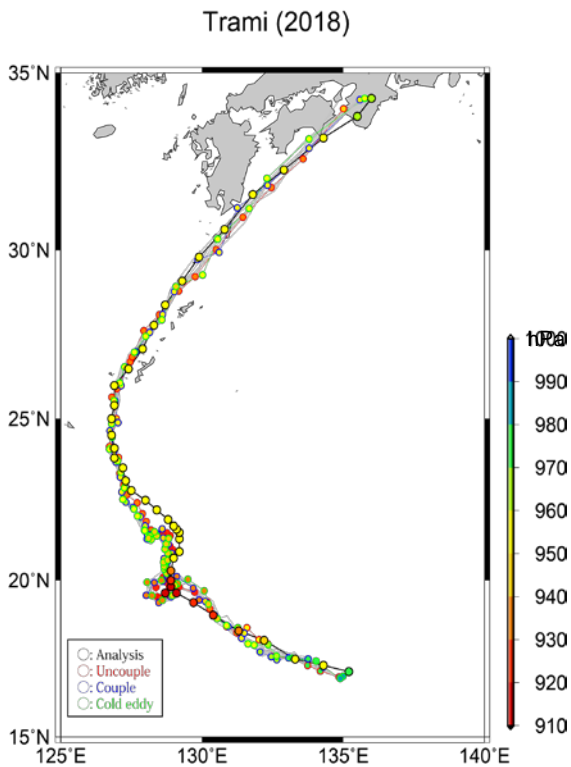


Figure 3. Results of track simulations in the A\_0923 (Uncouple), AWO\_0923 (Couple) and AWO\_cold (Cold\_eddy) experiments together with the best-track analysis.

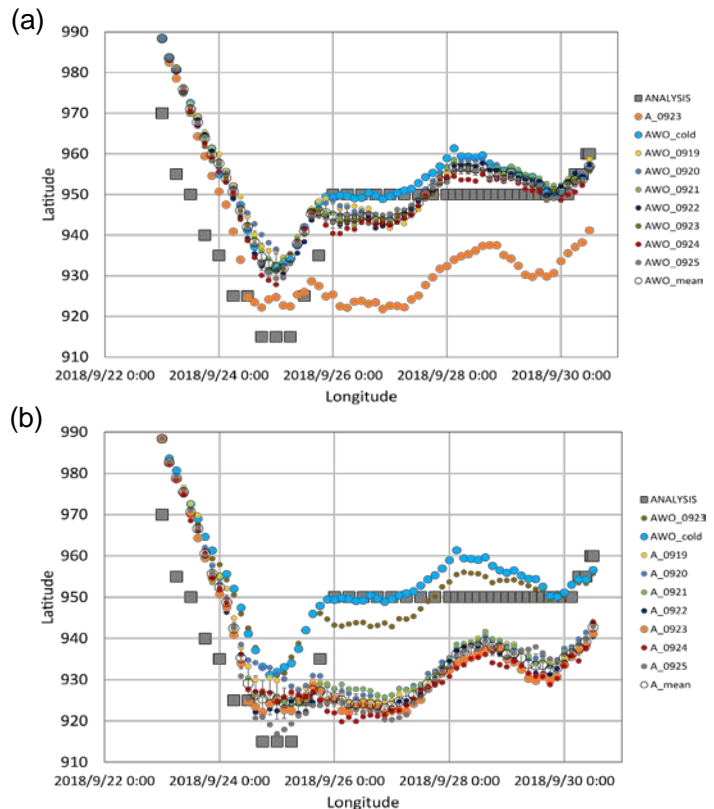


Figure 4. Time series of the best-track analyzed central pressure, simulated central pressure in the A\_0923, AWO\_0923 and AWO\_cold experiments together with (a) the simulated central pressures in the AWO series ensemble experiments and (b) those in the A series ensemble experiments.

The rapid decrease in the central pressure could not be simulated due to a large difference in central pressure at the initial time (Fig. 4). The simulated minimum central pressure was higher than the best track central pressure. The variation in the simulated central pressures in the AWO (Fig. 4a) and A (Fig. 4b) series experiments was smaller than the difference in the simulated central pressures between AWO\_0923 and A\_0923 experiments. In addition, the difference in the simulated central pressures between AWO\_0923 and AWO\_cold became large after 12UTC on 25 September due to the effect of artificial cold eddy. This suggests that the intensity forecast could be improved when the oceanic cold eddy was embedded in the initial oceanic condition. In other words, the intensity forecast errors resulted from errors in ocean analysis data currently used in this study.

#### 4. Concluding remarks

While the number of sea surface temperature observations from satellites is increasing, in situ observations in the upper ocean are still extremely sparse, particularly in storm areas. When a storm passes over oceanic cold eddies, the amount of storm-induced decreases in sea surface temperature becomes larger and thereby the development of the storm is suppressed. Without the effects of oceanic cold eddies and ocean coupling, the errors in typhoon intensity forecast will increase due to the overdevelopment of the intensity particularly when the moving speed of the typhoon is slow. Also, it is necessary to analyze storm-induced sea surface cooling more accurately in the sea surface temperature analysis. In this study, the Merged Satellite and In-situ Data Global Daily Sea Surface Temperatures (MGDSST) dataset (Kurihara et al., 2006) was used. The improvement of MGDSST is desirable to improve the typhoon intensity forecast.

#### References

Ito, K. et al. (2018). Analysis and Forecast Using Dropsonde Data from the Inner-Core Region of Tropical Cyclone Lan (2017) Obtained during the First Aircraft Missions of T-PARCII. SOLA, 14, 105-110.  
 Kurihara, Y., T. Sakurai, and T. Kuragano (2006). Global daily sea surface temperature analysis using data from satellite microwave radiometer, satellite infrared radiometer and in-situ observations (in Japanese). Wea. Service Bull., 73, 1-18.  
 Wada, A., N. Kohno and Y. Kawai (2010). Impact of wave-ocean interaction on Typhoon Hai-Tang in 2005. SOLA, 6A, 13-16.  
 Wada, A., S. Kanada, and H. Yamada (2018). Effect of air-sea environmental conditions and interfacial processes on extremely intense typhoon Haiyan (2013). Journal of Geophysical Research: Atmospheres, 123, 10379-10405.

#### Acknowledgement

This work was supported by JSPS KAKENHI Grant Number JP15K05292 and JP17H02964.

# Comparison of J-OFURO remote-sensing based ocean flux data with numerical simulations by a coupled atmosphere-wave-ocean model in Typhoon Dujuan (2015) case

Akiyoshi Wada<sup>1</sup>, Hiroyuki Tomita<sup>2</sup>

<sup>1</sup>Meteorological Research Institute, Tsukuba, Ibaraki, 305-0052, JAPAN

<sup>2</sup>Institute for Space-Earth Environmental Research, Nagoya University, Furocho, Chikusa-ku, Nagoya, Aichi 464-8601, JAPAN

<sup>1</sup>awada@mri-jma.go.jp

## 1. Introduction

A third-generation data set developed by the Japanese Ocean Flux Data Sets with Use of Remote-Sensing Observations (J-OFURO) research project provides surface heat, momentum, freshwater fluxes, and related parameters over the global oceans (Tomita et al., 2019). The data set currently covers the years from 1988 to 2013 with a daily temporal resolution and a horizontal resolution of  $0.25^\circ$ . In addition, a preliminary data set is available from 2014 to 2015. It is expected that it will be possible to use this data set for typhoon and extreme weather research by realizing high resolution in space and time. On the other hand, ‘typhoon’ is a phenomenon in which time fluctuations shorter than one day are predominant, including its ocean response. It is thought to be difficult to represent four-dimensional overall phenomena by using a data set with one-day time resolution and  $0.25^\circ$  degree spatial resolution. Therefore, in order to evaluate the applicability of the J-OFURO version 3 (J-OFURO3) data set to typhoon research, data comparison was performed with numerical simulation results by a 2 km-mesh nonhydrostatic atmosphere model coupled with ocean-surface wave and multilayer-ocean models (Wada et al., 2010, 2018) in the case of Typhoon Dujuan (2015).

Dujuan is one of the typhoons that made landfall in Taiwan. According to the Regional Specialized Meteorological Center (RSMC) Tokyo best track analysis, Dujuan was generated at 21 UTC on 22 September in 2015 and moved west-northwestward. The central pressure reached 925 hPa at 00 UTC on 27 September around  $22.3^\circ\text{N}$  and  $127.5^\circ\text{E}$ . Around  $20.0^\circ\text{N}$  and  $130.0^\circ\text{E}$ , Dujuan underwent steady intensification and the storm-induced sea surface cooling occurred by passage of the storm (Figure 1). In this study, the initial time and integration period for the numerical simulation of Dujuan are 00 UTC on 23 September in 2015 and 120 hours with the time interval of 3 seconds. The Japan Meteorological Agency (JMA) global objective analysis with horizontal resolution of 20 km and the JMA North Pacific Ocean analysis with horizontal resolution of  $0.5^\circ$  were used for creating atmospheric and oceanic initial conditions and atmospheric lateral boundary conditions. For comparison, a numerical simulation was performed by a nonhydrostatic atmosphere model with the same initial and boundary conditions.

## 2. Method

Sea surface temperature ( $^\circ\text{C}$ ), surface wind speed ( $\text{m s}^{-1}$ ) and air-sea latent heat flux ( $\text{W m}^{-2}$ ) were used for comparing the J-OFURO3 data with the results of numerical simulations. The domain for the comparison covers the area from  $16$  to  $32^\circ\text{N}$  and  $122$  to  $138^\circ\text{E}$ . Around  $20.0^\circ\text{N}$  and  $130.0^\circ\text{E}$ , the location of the simulated storm was close to that of the best track although the northward bias was found west of  $130.0^\circ\text{E}$ . The comparison was made around  $20.0^\circ\text{N}$  and  $130.0^\circ\text{E}$  from 24 and 25 September in 2015 when the storm did not arrive at the location.

Sea surface temperature, surface wind speed and air-sea latent heat flux simulated by the coupled model were averaged over a  $0.25^\circ \times 0.25^\circ$  grid, corresponding to the horizontal resolution of the J-OFURO3 data set every 6 hours. The correlation between the simulation results and J-OFURO3 data was investigated for each element from 12 UTC 24 September to 06 UTC 25 September 2015, after correcting the difference of the location between the simulation and the best-track analysis although the difference was smaller than  $1^\circ$ .

## 3. Results

Figure 2a shows the horizontal distribution of J-OFURO3 sea surface temperature on 25 September. Sea surface cooling induced by Dujuan was found along the track. Figure 2b shows the horizontal distribution of sea surface temperature simulated by the coupled model. The sea surface cooling induced by Dujuan was also found after the passage of the typhoon. This result indicates that J-OFURO3 sea surface temperature can capture storm-induced sea surface cooling.

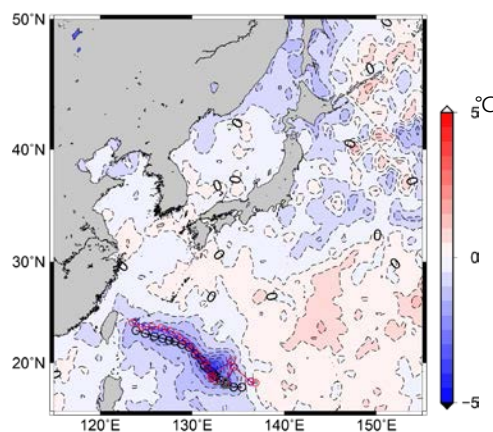


Figure 1. The best track (black circles) and simulated tracks (red circles by the uncoupled model and blue circles by the coupled model) and the difference in SST between before (-3 days) and after (+3 days) the passage of Dujuan derived from J-OFURO3 daily SST data.

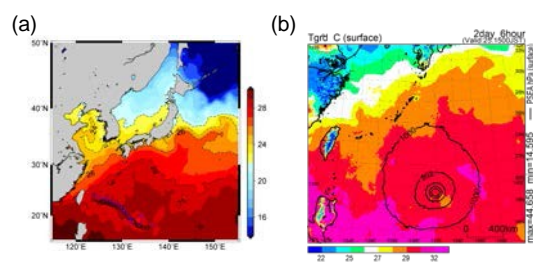


Figure 2. Horizontal distributions of (a) J-OFURO3 daily sea surface temperature on 25 September with the tracks shown in Fig. 1 and (b) simulated sea surface temperature (colors) at 06UTC (15JST) on 25 September with sea-level pressure at the contour interval of 8 hPa.

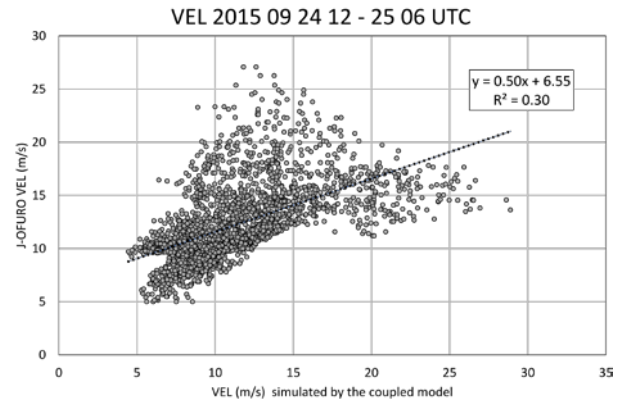
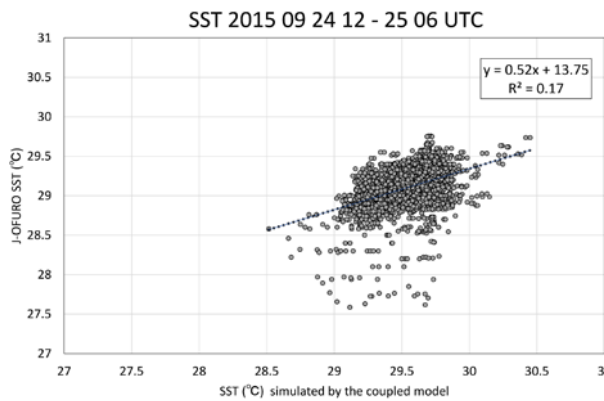


Figure 3. Correlation, simple linear regression model and coefficient of determination between J-OFURO3 data and simulation results for (a) sea surface temperature and (b) surface wind speed from 12 UTC on 24 September to 06 UTC on 25 September in 2015.

Figure 3 shows a scatter diagram, simple linear regression model and square of correlation coefficient between J-OFURO3 data and simulation results for sea surface temperature (Fig. 3a) and surface wind speed (defined by simulated wind speed at 10-m height) (Fig. 3b) from 12 UTC on 24 September to 06 UTC on 25 September in 2015. Although the coefficient of determination was relatively small, both correlation coefficients were significant at a significant level higher than 99.999% based on a  $p$ -value. However, the result also shows that there were positive biases in both simulated sea surface temperature and surface wind speed. The positive bias for sea surface temperature was possibly caused by the occurrence of TC-induced sea surface cooling after 06 UTC on 25 September.

The positive bias for surface wind speed was possibly caused by the following factors: Satellite wind observations could not capture high surface winds in the vicinity of a storm. Otherwise, the inner-core radial wind profile differed between the J-OFURO3 surface wind data and simulated surface wind speeds. In addition, the simulated Dujan moved westward, while the J-OFURO3 surface wind data cannot include the variation on a time scale shorter than a day.

Figure 4 shows a scatter diagram, simple linear regression model and coefficient of determination between J-OFURO3 data and simulation results for air-sea latent heat flux. The correlation coefficient was also significant at a significant level higher than 99.999% based on a  $p$ -value. The positive bias of simulated air-sea latent heat flux was caused by the positive biases of both sea surface temperature and surface wind speed. In fact, the slope of the linear regression model for air-sea latent heat flux (0.25) was almost the same as that for sea surface temperature (0.52) times that for surface wind speed (0.5). It should be noted that there were some grids where the J-OFURO3 air-sea latent heat flux was higher than the simulated one. This means that the J-OFURO3 could capture high air-sea latent heat flux in the vicinity of the storm although the location and inner-core structure of the typhoon differed between J-OFURO3 data and simulation results due to the difference of spatial and temporal resolution.

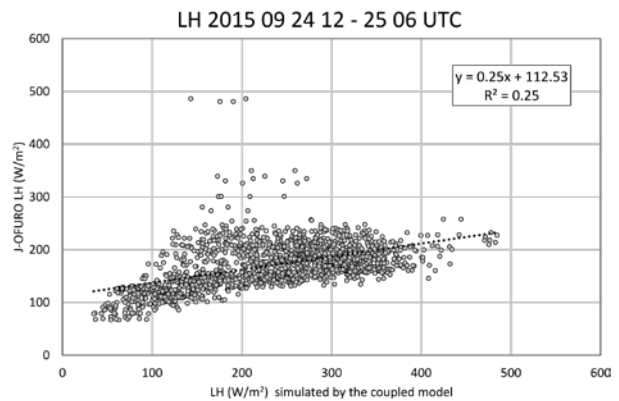


Figure 4. Same as Fig. 3 except for air-sea latent heat flux.

#### 4. Future subjects

J-OFURO3 air-sea sensible and latent heat fluxes are determined by not only sea surface temperature and surface wind speed, but also surface air temperature, surface specific humidity and exchange coefficients. Comparison of these elements simulated by the coupled model should be made with the J-OFURO3 data, separately. The results of the comparison will lead to the development of the coupled model in the future.

#### References

- Tomita, H. et al. (2019). An introduction to J-OFURO3, a third-generation Japanese ocean flux data set using remote-sensing observations. *Journal of Oceanography*, 75, 171-194.
- Wada, A., N. Kohno and Y. Kawai (2010). Impact of wave-ocean interaction on Typhoon Hai-Tang in 2005. *SOLA*, 6A, 13-16.
- Wada, A., S. Kanada, and H. Yamada (2018). Effect of air-sea environmental conditions and interfacial processes on extremely intense typhoon Haiyan (2013). *Journal of Geophysical Research: Atmospheres*, 123, 10379-10405.

#### Acknowledgements

This work was supported by JSPS KAKENHI Grant Number 18H03737.